Journal of Membrane Science 449 (2014) 15–26

Contents lists available at ScienceDirect

Journal of Membrane Science

journal homepage: www.elsevier.com/locate/memsci

Nanocomposites films based on soy proteins and montmorillonite processed by casting

Ignacio Echeverría [a], Patricia Eisenberg [b], Adriana N. Mauri [a,*]

[a] Centro de Investigación y Desarrollo en Criotecnología de Alimentos (CIDCA-CCT La Plata-CONICET)—Facultad de Ciencias Exactas, Universidad Nacional de La Plata (UNLP), Calle 47 y 116S/N°, B1900AJJ La Plata, Buenos Aires, Argentina
[b] Centro de Plásticos, Instituto Nacional de Tecnología Industrial (INTI), Avenida General Paz 5445, B1650KNA San Martín Buenos Aires, Argentina

ARTICLE INFO

Article history:
Received 25 February 2013
Received in revised form
5 July 2013
Accepted 4 August 2013
Available online 30 August 2013

Keywords:
Bionanocomposites
Soy proteins
Montmorillonite
Casting
Biodegradable films

ABSTRACT

In this work the effect of montmorillonite (MMT) addition to soy-protein-based films on the physicochemical properties of the resulting nanocomposites was studied and the structure–function relationship of these materials and the changes in phase structures, due to different interactions among the material components were analyzed. Flexible nanocomposite films consisting in a soy-protein (SP) matrix supplemented with different concentrations of montmorillonite (MMT) up to 10 g/100 g of SP were prepared by the casting technique. The resulting films were homogeneous, yellowish, and transparent and indistinguishable visually from films of pure protein. The process used for film formation—involving mechanical agitation and ultrasonication, in combination with the intrinsic affinity of MMT for the SPs—favors the dispersion of the clay so as to reach a high degree of intercalation into the protein matrix with consequent exfoliation of the layers of MMT among the proteins (verified by both transmission electron microscopy and X-ray diffraction). The efficient dispersion and distribution of the MMT laminas within the films generated a significant strengthening of the nanolayer that was evident in the observed resistance to breakage; modulation of elasticity; and decrease in extension, moisture content, solubility, and permeability to water vapor. In the presence of MMT, the disulfide bridges in the SPs play a critical role in the stabilization of the protein matrix, whereas in the films composed of proteins alone the residues capable of participating in hydrogen bonding would be involved in other types of highly stabilizing interactions.

1. Introduction

In recent years layered silicate-polymer nanocomposites have constituted a center of academic and industrial attention since those end materials frequently exhibit improvements in molecular barrier properties and thermal and mechanical characteristics in comparison to pure polymers [1–4]. Moreover, these nanoreinforcements are environmentally friendly, abundant in nature, and inexpensive. Diverse polymeric matrices have been used to form nanocomposites with the aluminum-silicate mineral montmorillonite (MMT) from those consisting in nonbiodegradable synthetic polymers—such as nylon [5,6], polystyrene [7,8], and polypropylene [9] to biopolymers—such as polylactide [10], starch [11–16], and proteins [17–21].

These improvements reported in nanocomposites reinforced by MMT were more pronounced when the clay layers were uniformly dispersed within the polymeric matrix to form an intercalated and thus exfoliated structure instead of forming extrinsic aggregates or tactoids [3]. The dispersion of the MMT in a polymeric matrix depends on the process used in the preparation of the nanocomposite, the nature of both the polymer and the clay, and finally the interaction between those two integral components. As layers of silicates are in the order of 1 nm and have very high aspect ratios (*e.g.* 10–1000), when a few weight percent of clay is properly dispersed throughout the matrix, a much higher surface area for polymer–filler interactions is created than for conventional composites [3].

In particular, the reported improvements in barrier properties (against oxygen or water) of the polymeric materials with minimal of clay incorporated in the formulation [22,23] have awakened an interest in the application of nanoclays to the production of food packaging, either flexible or rigid. The complete dispersion of clay layers in a polymer must optimize the number of strengthening elements available to support a load and avoid cracks in the material, improving the mechanical properties. In addition, the clay layers generate a tortuous pathway through which the permeable elements have much greater difficulty in penetrating the nanocomposite.

* Corresponding author. Tel./fax: +54 221 4890741.
E-mail address: anmauri@quimica.unlp.edu.ar (A.N. Mauri).

0376-7388/$ - see front matter © 2013 Elsevier B.V. All rights reserved.
http://dx.doi.org/10.1016/j.memsci.2013.08.006

Agro-proteins are an attractive alternative to synthetic plastic made from non-renewable resources that can be a hazard to the environment [24] at least in some applications. Protein films generally exhibit excellent barrier properties against oxygen, lipids, and aroma, poor mechanical properties and high water vapor permeability [25–27]. This behavior should be attributed to the inherent hydrophilic nature of proteins, and to the presence of plasticizers (*e.g.* glycerol) in the formulation that are usually added to avoid chipping or cracking of the film during subsequent handling and storage [28]. These properties along with their biodegradability makes these materials interesting for their use in short-lived products such as food packaging.

Among proteins, those from soybeans have been extensively studied in order to develop films that are biodegradable, and even edible, because soy proteins are among the most abundant and economical and furthermore can be recovered as a recyclable by-product of the vegetable-oil industry [29].

Numerous studies have been reported and reviewed by Song et al. [30] considering different alternatives to improve the mechanical properties and to decrease the water sensibility of soy proteins based materials thus extending their usefulness. They included physical chemical and/or enzymatic treatments on proteins and film forming dispersions, the preparation of materials from blends of proteins with other biopolymers, the addition of lipids, fibers, nanoreinforcements and other compounds that could activate films with other properties, such us antimicrobial or antioxidant ones.

Because of the hydrophilic nature of both the soy proteins and natural sodium MMT, the dispersion of both materials in water and subsequent generation of nanocomposites through the process of *casting* becomes possible.

The aim of this work was therefore to study the effect of MMT addition to soy-protein-based films on the physicochemical properties of the resulting nanocomposites and to analyze the structure–function relationship of these materials and the changes in phase structures due to different interaction between the material components (proteins, montmorillonite, glycerol and water).

2. Experimental

2.1. Materials

Soy protein isolate (SPI; SUPRO 500-E) was generously provided by The Solae-Company (Brasil). The protein content of SPI, as measured by the Kjeldahl method, was 85 ± 2% (w/w, dry weight; N × 6.25). Sodium MMT without organic modification (Cloisite®Na^+)—supplied by Southern Clay Products (USA)—has a cation-exchange capacity of 92.6 meq/100 g clay, a typical interlayer distance of 11.7 Å, a bulk density of 2.86 g cc^{-1}, and a typical particle-size distribution between 2 and 13 μm. Glycerol (p.a., Anedra) was used as a film plasticizer.

2.2. Film preparation

Five gram of SPI was dispersed in 80 ml of distilled water at room temperature by magnetic stirring and the pH of the dispersion adjusted to 10.5 with 2 N NaOH. Different amounts of MMT powder (0, 0.125, 0.25, 0.375, and 0.5 g) plus 1.25 g of glycerol were likewise dispersed in 20 ml of distilled water for ≈1 h followed by sonication with a Sonics Vibra-cell model VCX 750 at 80% amplitude (Sonics & Materials, Inc., USA). The dispersions of SPI and MMT-glycerol were then mixed by stirring for 1 h at room temperature, and the resulting dispersed admixture centrifuged at 78 g for 5 min at room temperature in order to eliminate bubbles. Finally, the film-forming dispersions were cast onto polystyrene Petri dishes (64 cm^2) and dried in an oven at 60 °C for 3 h. The dry films were conditioned at 20 °C and 58% relative humidity in desiccators with saturated solutions of NaBr for 48 h before being peeled from the casting surface for characterization. Five MMT contents were studied: 0, 2.5, 5, 7.5, and 10 g MMT per 100 g SPI.

2.3. Rheological measurement of film forming dispersions

The apparent viscosity (η_{app}) and flow behavior of SPI-MMT film-forming dispersions at concentrations of 0, 2.5, 5, 7.5, and 10 g MMT per 100 g of SPI were evaluated in a ReoStress 600 rheometer (Termo Haake, Karlsruhe, Germany) with a 1-mm gap parallel-plate serrated sensor. The SPI-MMT filmogenic dispersions were maintained at 25 °C by a circulating water bath (Circulator DC50 Thermo Haake) connected to the jacket surrounding the sensor system during testing. The shear rate (D) was increased from 0 to 500 s^{-1} in 2 min, was maintained for 1 min and then decreased from 500 to 0 s^{-1} over a period of another 2 min. The η_{app} was calculated in the ascending curves at 300 s^{-1}. The flow (n) and consistency index (K) were determined after adjusting the empirical data according to the Ostwald de Waele rheological model (aka the Power-Law model):

$$\tau = K\dot{\gamma}^n, \tag{1}$$

where τ is the shear stress (Pa), K the consistency index (Pa s^n), and n is the flow-behavior index. This last parameter is a dimensionless number that measures the closeness to Newtonian flow; with a value of 1 indicating a Newtonian, higher than 1 a dilatant, and between 0 and 1 a pseudoplastic fluid.

2.4. Film thickness

Before testing, the film thickness was measured by a digital coating-thickness gauge (Check Line DCN-900, USA). Measurements for testing the mechanical and water-barrier properties were performed at nine different locations on the films. The mean thickness was used to calculate these physical properties.

2.5. Film color

Film colors were determined with a Minolta Chroma meter (CR 300, Minolta Chroma Co., Osaka, Japan). A Hunter Lab color scale was used to measure the degree of lightness (L), redness ($+a$) or greenness ($-a$), and yellowness ($+b$) or blueness ($-b$) of the films. The instrument was standardized by means of a set of three Minolta calibration plates. The films were measured on the surface of the white standard plate with color coordinates of $L=97.3$, $a=0.14$ and $b=1.71$. Total color difference (ΔE) was calculated from

$$\Delta E = \sqrt{(L_{film}-L_{\text{standard}})^2+(a_{film}-a_{\text{standard}})^2+(b_{film}-b_{\text{standard}})^2} \tag{2}$$

Values were expressed as the means of nine measurements on different areas of each film.

2.6. Opacity

Each film specimen was cut into a rectangular piece and placed directly in a spectrophotometer cell, and measurements were performed with air as the reference for transparency. A spectrum of each film was obtained in a UV–vis spectrophotometer (Beckman DU650, Germany). The area under the absorption curve from 400 to 800 nm was recorded and the opacity of the film (arbitrary units/mm) calculated by dividing the absorbance at 500 nm by the

film's thickness (mm) [31]. All determinations were performed in triplicate.

2.7. Moisture content

Small specimens of films (≈0.25 g) were collected after conditioning, cut, and weighed before and after drying in an oven at 105 °C for 24 h. Moisture-content values were determined in triplicate as the difference between the two weights for each film and were expressed as a percent of the original weight (American Society for Testing and Measurements [ASTM] D644-94, 1994).

2.8. Solubility

The solubility of films was determined in triplicate, according to the method proposed by Gontard et al. [32]. Three pieces of film (2 cm in diameter) were immersed in 50 mL distilled water, and the system was slowly stirred at room temperature (22–25 °C) for 24 h. After filtration of the samples (Whatman 1) the nonsolubilized material on the paper was dried in a forced-air oven (105 °C, 24 h) in order to determine the weight of the water-insoluble fraction as a percent of the total.

2.9. Water-vapor permeability (WVP)

WVP tests were conducted by the ASTM method E with certain modifications [33]. Each film sample was sealed over a circular opening of 0.00185 m^2 in a permeation cell that was subsequently stored at 20 °C in a desiccator. To maintain a 75% RH gradient across the film, anhydrous silica (0% RH_c) was placed inside the cell and a saturated NaCl solution (75% RH) in the desiccator. The RH therefore was always lower inside the cell than outside, and the water-vapor transport was accordingly determined from the weight gain of the permeation cell. When steady-state conditions were reached (after about 1 h), eight weight measurements were made over a period of 7 h. Changes in the weight of the cell were recorded and plotted as a function of time. The slope of each line was calculated by linear regression (Origin Pro 8.5 software) and the water-vapor-transmission rate was calculated from the slope (g H_2O s^{-1}) divided by the cell area (m^2). WVP (g H_2O/Pa s m) was calculated as

$$\mathrm{WVP} = \frac{\mathrm{WVTR}}{P_v^{H_2O}(RH_d - RH_c)A}d \tag{3}$$

where WVTR=the water-vapor-transmission rate, $P_v^{H_2O}$=vapor pressure of water at saturation (1753.35 Pa) at the test temperature (20 °C), RH_d=RH in the desiccator, RH_c=RH in the permeation cell, A=permeation area, and d=film thickness (m). Each WVP value represents the mean value of at least three samples taken from different films.

2.10. Sorption isotherms

The water-adsorption isotherms of the films were determined by the static method, through the use of saturated saline solutions (NaOH, LiCl, KCH_2COO $MgCl_2$, K_2CO_3, $MgNO_3$, $NaNO_2$, NaCl, KCl, $BaCl_2$, and $CuSO_4$) to obtain different RHs [34]. Film samples were then conditioned in desiccators having the desired RH (*i.e.*, 7, 11.2, 24.9, 33.2, 43.1, 54.4, 65.5, 75.4, 85.3, 90.7, 97.2%, respectively) and periodically weighed until three measurements of constant weight were obtained. The stable weight indicated that the films were equilibrated at the desired RH (after 21 days). The amount of water absorbed per gram of dry film (X_{eq}) was considered to be the difference between the initial and the final weights. The Guggenheim–Anderson–de Boer (GAB) model of Eq. (4) was used to fit the film-sorption-isotherm data:

$$X_{eq} = \frac{X_o\, K\, C a_w}{(1-Ka_w)(1-Ka_w+1-Ca_w)} \tag{4}$$

where X_{eq} is the humidity content of the sample (dry base) in the equilibrium (g H_2O g^{-1} dry film) at a given aqueous activity (a_w), X_o is the moisture content (dry base) of the monolayer (g H_2O g^{-1} dry film), C is the Guggenheim constant associated with the sorption heat of the monolayer, and K is the constant associated with the sorption heat of multilayers. The parameters of the model (X_o, K, and C) were determined by the quadratic regression of a_w/X_{eq} versus a_w by means of the OriginPro 8 SR0 v8.0724 software (OriginLab Corporation, USA).

2.11. Solubility and diffusion coefficients of water in the film

The solubility coefficient of water in the films at 20 °C and 75% RH, β (g H_2O/Pa g of dry film), was determined using Eq. (5), according to Larotonda et al. [35], based on the experimental water sorption isotherms, GAB model and Eq. (4).

$$\beta = \frac{C\,K\,X_o}{P_v^{H_2O}}\left[\begin{array}{l}\frac{1}{[(1-K\ a_w)(1-K\ a_w+C\ K\ a_w)]} \\ -\frac{a_w}{[(1-K\ a_w)(1-K\ a_w+C\ K\ a_w)]^2} \\ [-K(1-K\ a_w+C\ K\ a_w)+(1-K\ a_w)(-K+C\ K)])]\end{array}\right] \tag{5}$$

The coefficients of water diffusion (D_{ef}) through the films at 20 °C and 75% RH were determined from data on water vapor permeability (WVP), solubility coefficient of water in the film (β) and film density (ρ^s), using the following equation.

$$D_{ef} = \frac{\mathrm{WVP}}{\rho^s \beta} \tag{6}$$

2.12. Mechanical properties

The tensile strength, Young's modulus, and elongation at break of the films were determined following the procedures outlined in the ASTM methods D882-91 with an average of seven measurements taken for each film and with at least two films per formulation. The films were cut into 6-mm by 80-mm strips that were mounted between the grips of the texture analyzer (TA.XT2i, Stable Micro Systems, Surrey, England). The initial grip separation was set at 50 mm and the crosshead speed at 0.5 mm/s. The tensile strength (σ=force per initial cross-sectional area) and elongation at break (ε) were determined directly from the stress–strain curves through the use of OriginPro 8 SR0 v8.0724 software (OriginLab Corporation, USA), and Young's modulus (E) was obtained from the slope of the initial linear portion of that curve.

2.13. Differential scanning calorimetry (DSC)

The glass-transition temperature (T_g) of films and the degree of denaturation of protein products were determined by differential scanning calorimetry, with a DSC TA 2010 calorimeter Model Q100 V9.8 Build 296 (TA Instrument, New Castle, DE, USA) controlled/regulated by a TA 5000 module with a quench-cooling accessory. The temperature and heat-flow calibration of the equipment were carried out according to ASTM indications, with lauric and stearic acids plus indium as standards. Hermetically sealed aluminum pans containing 10–15 mg of film were prepared and scanned at 10 °C/min over the range −100 to 220 °C in order to determine the value of T_g. This parameter is defined as the inflexion point of the base line, caused by the discontinuity of the specific heat of the sample and in these experiments was calculated by means of the Universal Analysis V4.2E software (TA Instruments, New

Castle, DE, USA). All the assays were performed in at least duplicate.

2.14. X-ray diffraction

X-ray diffraction was carried out on a X'Pert Pro diffractometer (PANalytical, USA) equipped with a Cu Kα radiation source ($\lambda = 0.154$ nm). The voltage and the current used were 40 kV and 40 mA, respectively. The diffraction data were collected from $2\theta = 1.5–10^{\circ}$ in a fixed-time mode with a step interval of 0.01°. The basal spacing of the silicate layer, d, was calculated by means of the Bragg equation:

$$\lambda = 2d \sin \theta \quad (7)$$

where θ is the diffraction position and λ is the wavelength.

2.15. Transmission electron microscopy

Small pieces of film (0.5 mm^2) were fixed in 2.5% (v/v) glutaraldehyde in Sorenssen buffer (pH 7.2), washed in the same buffer three times for 30 min each, and then postfixed in 2% (w/v) OsO_4 for 1 h. The samples were next washed with distilled water three times for 30 min each, serially dehydrated in aqueous acetone (25%, 50%, 75%, and 100% [3 ×]), and finally embedded in Spurr Resin (1:2, 2:2, 2:1) and pure resin overnight. Polymerization was carried out at 70 °C overnight. The embedded samples were sectioned with an LKB ultramicrotome. The grids were stained with uranyl acetate (1 min) and lead-citrate (40 min) and observed with a JEOL 100CXII (Tokyo, Japan) transmission electron microscope at 80 kV.

2.16. Differential solubilization of proteins

The protein solubilization of the films was determined according to the method described by Mauri and Añón [36], with certain modifications. Pieces of films (≈ 50 mg) were weighed and placed in a tube containing 1 ml of water or buffer. Five different buffer systems, all at pH 7.5, were used: (a) 0.1 M phosphate buffer containing 0.1 M NaCl (PB Buffer); (b) PBD Buffer: PB Buffer plus 0.1% (w/v) sodium dodecyl sulfate (SDS; Anedra, Argentina); (c) PBU Buffer: PB Buffer plus 6 M urea (Riedel-deHaën, Germany); (d) PBDU Buffer: PB Buffer plus 0.1% (w/v) SDS and 6 M urea, and (e) PBDUM buffer: PB Buffer plus 0.1% (w/v) SDS, 6 M urea, and 2.5% (v/v) mercaptoethanol (ME, Sigma-Aldrich, Germany). After the tubes were shaken for 24 h at 20 °C, the suspensions were centrifuged at 9000*g* for 20 min and the protein content in the supernatant determined by the Bradford assay [37]. Standard curves with bovine-serum albumin (Sigma-Aldrich Chemical Co., St. Louis, MO, USA) were constructed for each buffer. For each type of film, at least two samples from four independent film preparations were solubilized. The content of solubilizable protein was expressed as a percent of the total amount of protein in the film, as measured by the Kjeldahl method (Association of Official Agricultural Chemists [AOAC] 920.53).

2.17. Statistical analysis

Results were expressed as mean ± standard deviation, and the data were compared by analysis of variance (ANOVA). Means were tested with the Tukey's HSD (honestly significant difference) test for paired comparisons, at a significance level $p < 0.05$, through

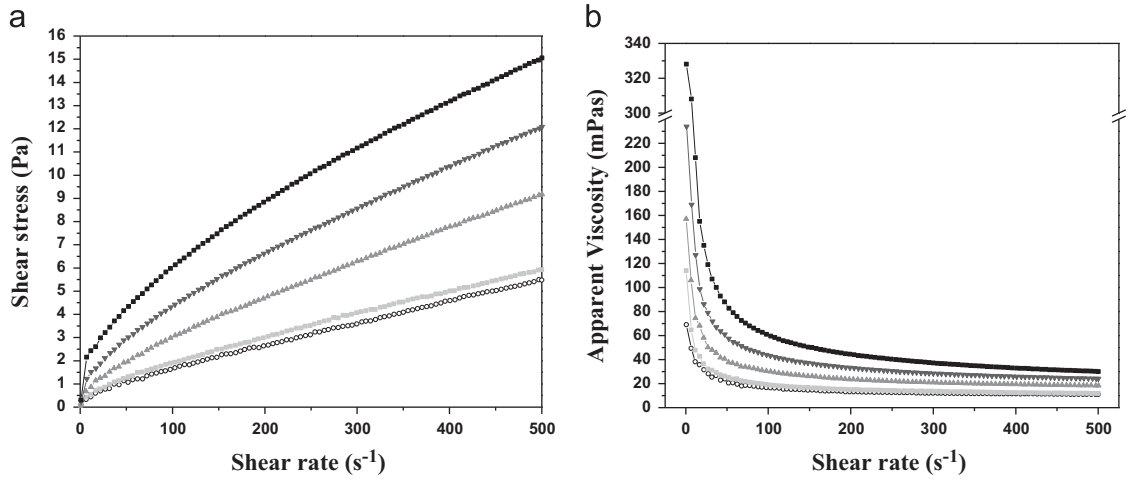

Fig. 1. Curves of (a) shear stress (Pa) and (b) apparent viscosity (MPa s) vs. shear rate (D) of filmogenic dispersions with increasing concentrations of montmorillonite (MMT): 0 (○), 2.5 (■), 5 (▲), 7.5 (▼), and 10 (■) g of MMT per 100 g of soy-protein isolate (SPI).

Table 1
Rheological characteristics of soy-protein (SPI) film-forming solutions in the presence of increasing contents of montmorillonite (MMT): Panel A: Index of consistency (K) and flow behavior (n); Panel B: Apparent-viscosity values calculated at shear rates (D) of 60, 300, and 500 s^{-1}.

MMT (g/100 g SPI)	A. Ostwald de Waele parameters			B. Apparent viscosity (mPa s)		
	K (Pa s^n)	n	r^2	$D = 60\ s^{-1}$	$D = 300\ s^{-1}$	$D = 500\ s^{-1}$
0	0.055 ± 0.005^a	0.747 ± 0.003^e	0.9993	20.6 ± 0.8^a	12.7 ± 1.1^a	11.4 ± 0.6^a
2.5	0.072 ± 0.002^b	0.709 ± 0.007^d	0.9993	23.3 ± 0.8^b	13.7 ± 0.1^a	12.0 ± 0.2^a
5	0.125 ± 0.004^c	0.686 ± 0.006^c	0.9993	36.6 ± 0.5^c	20.7 ± 0.3^b	18.3 ± 0.5^b
7.5	0.198 ± 0.006^d	0.646 ± 0.000^b	0.9992	48.7 ± 1.2^d	26.0 ± 0.7^c	22.2 ± 0.5^c
10	0.369 ± 0.009^e	0.588 ± 0.003^a	0.9992	70.5 ± 0.8^e	34.8 ± 0.3^d	28.9 ± 0.1^d

Value for each film is the mean ± standard deviation. Values with different superscript letters are significantly different ($p < 0.05$) according to the Tukey test.

the use of the OriginPro 8 SR0 v8.0724 software (OriginLab Corporation, USA).

3. Results and discussion

3.1. Rheologic characterization of film-forming dispersions

Fig. 1 and Table 1 summarize the rotational rheologic characteristics of the SPI and SPI-MMT filmogenic dispersions. The experimental values for shear stress as a function of the shear rate conformed satisfactorily to the model of Ostwald de Waele (Eq. (1)), thus yielding correlation coefficients greater than 0.999 in all instances. All the dispersions of SPI and SPI-MMT exhibited a pseudoplastic flow behavior ($K>0$, $0<n<1$, $\tau_0=0$, with τ_0 being the yield stress; Table 1) and as such manifested decreasing apparent-viscosity values upon increases in the deformation-velocity gradient (Table 1 and Fig. 1). The pseudoplastic behavior of the dispersions became progressively pronounced with increases in the clay content of the formulation since those increments produced a decline in the flow-behavior index (n) along with a concomitant increase in the viscosity of the dispersions (*i.e.*, indicated by higher values of K and of the measured apparent viscosity). Although this latter elevation was seen over the entire range of shear rates analyzed, the increment in viscosity in parallel with the increasing content of clay was more pronounced at low shear-rate values.

An increment in the apparent viscosity at low shear rates as a result of the introduction of clay into the formulation of nanocomposites has been previously reported in synthetic-polymer solutions [1,38,39]. This behavior was attributed to (i) changes in the preferential orientation of the silicates within the layers along with the conformation of the polymer in parallel to the direction of the flow during the shearing and (ii) the interactions between the MMT and the polymer chains. In addition, formulations involving a base of wheat-gluten proteins along with MMT have likewise been reported [18]. That the addition of MMT to filmogenic dispersions increases the content of solids—with not all of those being completely soluble—is furthermore noteworthy since that change might also explain, at least in part, the increment observed in the apparent viscosity (for a fixed shear rate D).

Moreover, that the filmogenic dispersions containing up to 10 g of MMT per 100 g of SPI in the present work exhibited adequate viscosities (between 16 and 61 mPa s at a $D=100\ s^{-1}$) so as to enable bubble removal from the dispersions upon light centrifugation also deserves mention in addition to the maintenance of an adequate fluidity for pouring the dispersions during the casting step. We were unable to obtain homogeneous films at clay concentrations in excess of 10 g of MMT per 100 g of SPI since at higher concentrations the viscosities of the dispersions increased (up to 87 and 120 mPa s, at a $D=100\ s^{-1}$, for concentrations of 12.5 and 15 g of MMT per 100 g of SPI, respectively) to the extent that the lack of fluidity complicated at once the admixture, the removal of bubbles, and the casting; thus resulting in the continued presence of residual bubbles in the final films.

3.2. Film characterization

3.2.1. Appearance

The nanocomposite films obtained by casting were homogeneous, translucent, and yellowish with a general visual appearance similar to the control unalloyed protein films (Fig. 2). Furthermore, all the films had similar thicknesses (Table 2).

Table 2 gives the optical properties (*e.g.*, color and opacity) of the protein films and the nanocomposites. With increasing concentrations of clay the luminosity was seen to decrease (the parameter L declines), the parameter a became progressively more negative (indicating the shift to a greenish cast), and the parameter b attained more positive values (denoting the assumption of a yellowish hue) to give an overall tone tending toward the greenish-yellow. These shifts were accordingly reflected in the progressive increase in the parameter ΔE (color differential) with added amounts of MMT in the formulation. Furthermore, that higher concentrations of MMT resulted in a lower level of film opacity would be consistent with a good degree of affinity between the soy proteins and the clay particles. It could be possible to achieve a better dispersion of protein in water in the presence of clay and plasticizer, preventing the formation of microaggregates that can be formed in the case of soybeans and glycerol and might scatter light, reducing transparency and increasing opacity. These results also suggest that protein matrix would be stabilized by different types of interactions in the presence or absence of MMT, and these new interactions would give different molecular levels of aggregation, which finally allow slight higher transparency in the nanocomposite films.

It seems that MMT layers would be exfoliated in soy protein matrix in an important degree. Petersson and Oksman [40] suggest that the degree of exfoliation and volume fraction of the nanoreinforcement had a large influence on the transmittance of UV and visual light, as they reported that no reduction in the amount of light being transmitted through the nanocomposite films is an indication that the nanoreinforcements are fully exfoliated, due to a transparent matrix containing low volume percent fully exfoliated nanoreinforcement is said to obtain good optical clarity. As a result there should not be a large difference in the amount of light being transmitted through the nanocomposite films compared to pure matrix.

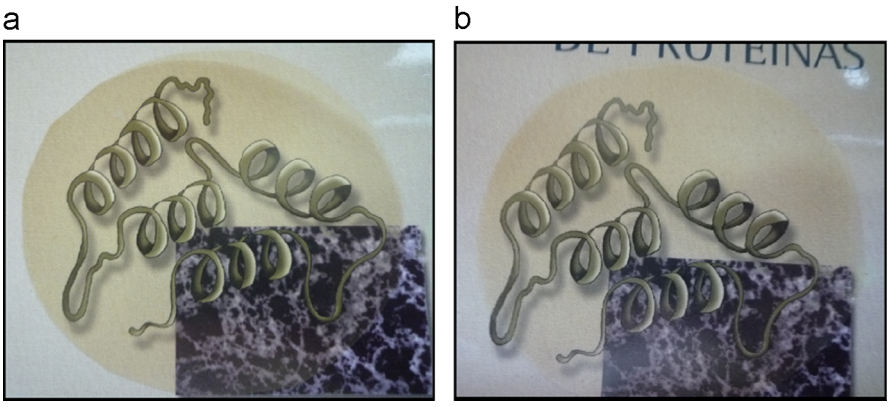

Fig. 2. Appearance of soy-protein films (a) without montmorillonite (MMT) and (b) with 5 g of MMT per 100 g of soy-protein isolate (SPI).

Table 2
Thickness, color parameters (*L*, *a*, *b*, DE), and opacity of soy-protein-isolate (SPI) films with different amounts of montmorillonite (MMT).

% MMT (g MMT/100 g SPI)	**Thickness (μm)**	**Hunter-lab color parameters**				**Opacity (UA mm^{-1})**
		L	***a***	***b***	**Δ*E***	
0	74.7 ± 8.5^{a}	87.02 ± 0.17^{c}	-0.35 ± 0.11^{a}	11.10 ± 0.48^{a}	13.93 ± 0.39^{a}	2.3 ± 0.02^{c}
2.5	82.4 ± 6.2^{a}	87.10 ± 0.34^{c}	$-0.51 \pm 0.12^{a,b}$	11.54 ± 0.63^{a}	14.18 ± 0.63^{a}	ND
5	80.8 ± 5.5^{a}	86.14 ± 0.73^{b}	-0.69 ± 0.29^{b}	13.52 ± 2.29^{b}	16.30 ± 2.18^{b}	1.7 ± 0.1^{b}
7.5	84.9 ± 6.9^{a}	85.66 ± 0.16^{b}	-0.84 ± 0.03^{c}	14.65 ± 0.30^{b}	17.43 ± 0.30^{b}	ND
10	89.0 ± 9.9^{a}	84.76 ± 0.52^{a}	-1.15 ± 0.14^{d}	17.52 ± 1.41^{c}	20.23 ± 1.43^{c}	1.2 ± 0.1^{a}

Values for each film are means ± standard deviations. Values with different superscript letters in a given column are significantly different ($p < 0.05$) according to the Tukey test. ND=not determined.

Table 3
Moisture content, solubility, water-vapor permeability (WVP), water-solubility coefficient (β), effective diffusivity (D_{ef}), and glass transition (T_g) of films prepared from soy proteins and soy proteins with different percentages of montmorillonite (MMT).

MMT (g/100 g SPI)	**Moisture content** (%)	**Solubility** (%)	**WVP $\times 10^{-11}$** (g seg^{-1} m^{-1} Pa^{-1})	**$\beta \times 10^{-4}$** (g H_2O/Pa g dry film)	**$D_{ef} \times 10^{-12}$** (m^2 s^{-1})	**T_g**	
						T_{g1} (°C)	**T_{g2} (°C)**
0	21.74 ± 0.84^{d}	51.15 ± 0.81^{c}	12 ± 0.8^{c}	6.3	2.15	-74.4 ± 8.9	-40.6 ± 0.1^{a}
2.5	20.43 ± 0.29^{c}	39.90 ± 2.62^{b}	11 ± 0.3^{c}	ND	ND	—	-39.6 ± 0.9^{a}
5	18.64 ± 0.09^{b}	39.46 ± 1.65^{b}	6.8 ± 0.2^{b}	6.0	1.39	—	-39.8 ± 1.4^{a}
7.5	17.26 ± 0.80^{a}	33.18 ± 0.56^{a}	$5.0 \pm 0.6^{a,b}$	ND	ND	—	-39.7 ± 1.3^{a}
10	16.95 ± 0.81^{a}	33.25 ± 0.12^{a}	3.2 ± 0.9^{a}	5.4	0.47	—	-40.7 ± 0.1^{a}

Values for each film are means ± standard deviations. Values with different superscript letters in a given column are significantly different ($p < 0.05$) according to the Tukey test. ND=Not determined.

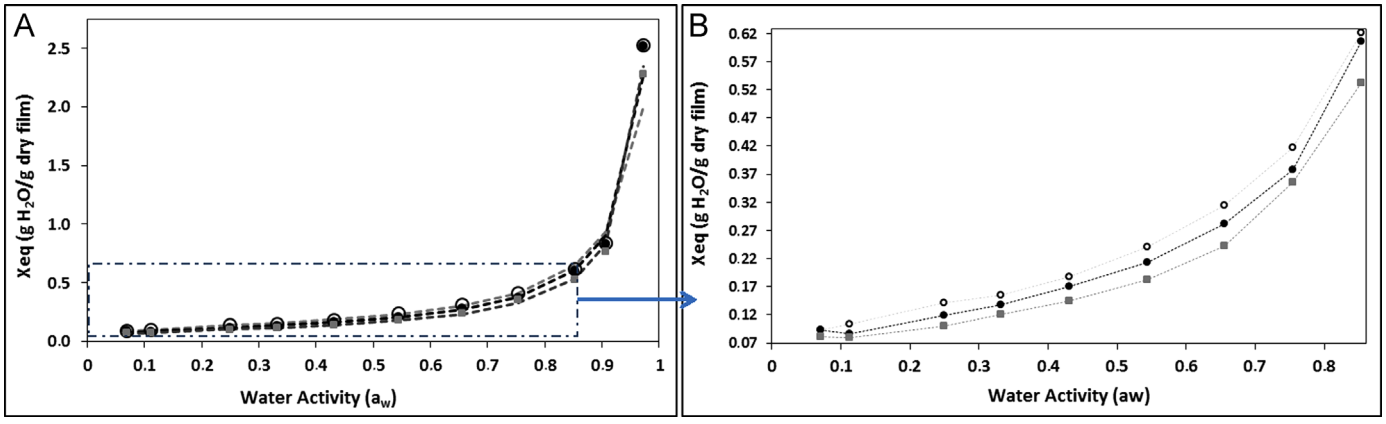

Fig. 3. (A) Sorption isotherms of films prepared with soy protein (○), 5 (●) and 10 (■) g MMT/100 g SPI. Filled symbols correspond to experimental data, and dotted lines indicate data adjusted with the GAB model. (B) Magnified sorption isotherms from A.

The significant quantitative differences in the parameters analyzed were not, however, reflected in qualitative changes in the films' visual appearances (Fig. 2) since those nanocomposites maintained the same yellowish cast, for all amounts of added MMT that characterized the films of pure soy protein [41]. That retained transparency and negligible additional coloration would favor the application of these materials in the use of packaging where the manufacturer or producer would be interested in an at least partial visibility of the product, a condition of particular relevance to the wrapping of foodstuffs.

3.2.2. *Water susceptibility*

The susceptibility to water characteristic of protein films owing to the hydrophilic nature of those macromolecules could be considered one of the most disadvantageous properties with respect to certain applications and a feature that most discriminates these biopolymers from the more frequently used synthetic polymers. Thus, an increased resistance to water in the former is one of the most sought after modifications for their more widespread practical use. Table 3 gives the moisture content and solubility in water of films composed of soy protein alone and of the nanocomposites.

Increasing amounts of MMT in the film formulation was accompanied by a progressive diminution in the percent-moisture content down to a value for the film with 10 g of MMT per 100 g of SPI that represented only 22% of the moisture of the unalloyed soy-protein film. Because MMT in its natural state could be considered to possess a certain degree of hydrophilicity [42,43] and the capacity to interact with water through hydrogen bonding [44], the decrease in water content observed in the nanocomposite films would suggest that the resulting affinity between the protein and the clay and between glycerol and the clay leaves fewer interaction sites available for the retention of water. Since, however, water acts as a form of plasticizer within the protein matrix [28], this decline in the moisture level of the nanocomposites must

be kept in mind when analyzing the functionality of the resulting materials.

The solubility in water of these films also became progressively reduced with increasing MMT contents in the formulation, reaching a value representing only 65% of the solubility of the pure-protein film with the nanocomposite of 10 g of MMT per 100 g of SPI. The same effect had been reported by other authors [45–47] with MMT added to films composed of agar, chitosan, and cotton-carboxymethylcellulose: they attributed those results to the formation of hydrogen bonds between the clay and the hydroxyl groups of those different matrices. After solubility experiments, the nanocomposite films did not lose their integrity and were handable, but they just suffered a swelling without getting a gel state. Otherwise, the soy protein films lost their integrity.

Fig. 3 shows the sorption isotherms of the protein films analyzed. All the isotherms had a sigmoidal shape ($C > 2$), increasing asymptotically to infinity when a_w approached 1, the latter feature being typical of products rich in proteins or starch [48]. Although the nanocomposite films exhibited lower water-absorption values than the soy-protein controls over the entire range of aqueous activities, those differences were more pronounced in environments with elevated levels of RH.

The GAB model was adequate for describing mathematically the sorption isotherms ($r^2 \approx 0.99$), but the experimental data diverged from the model at high RH values ($a_w > 0.9$) since in this zone the sorbate exhibits properties of pure water, whereas one of the GAB's initial assumptions is of physical adsorption in multilayers.

Table 4 lists the parameters obtained upon modifying the experimental data to correspond to the GAB model. The high r^2 values confirmed that the equation was a good model for representing the experimental data. The moisture content in the monolayer (X_o) decreased with increasing amounts of nanoclay, probably because of the strong hydrogen bonding between the hydroxyl groups of the soy proteins and the MMT that rendered the former inaccessible for interaction with water and thus gave the nanocomposites a progressively increasing hydrophobicity. The water-adsorption values found with the soy-protein films in this study were similar to those reported by other authors [49,50], but at the present time we have been unable to find literature data on sorption isotherms for nanocomposite films containing protein and MMT.

Since one of the functions of a film to be used in packaging is to minimize the transfer of moisture to a food from the surrounding atmosphere or between two components of a heterogeneous product of differing moisture levels; the evaluation of a film's permeability to water vapor is critical, and that parameter is always maintained at as low a value as possible. The WVP data for the control film with soy protein alone is typical of protein-containing films [36,48,51–54] (Table 3). The addition of clay to the formulation produced a significant drop in that property, especially for MMT contents in excess of 5 g per 100 g of SPI (at which concentration a decline of 43% in the WVP was observed). Although at 10 g of MMT per 100 g SPI the WVP of 3.2×10^{-11} g/m s Pa was nearly an order of magnitude lower than that of the control film (at 12×10^{-11} g/m s Pa) and was, moreover, well within the range for certain synthetic films such as cellophane (at 8.4×10^{-11} g/m s Pa); nevertheless, those minimal values were still higher than the figures reported for the synthetic products most frequently used commercially—*e.g.*, polypropylene at 6.5×10^{-13}, polyvinyl chloride at $0.7–2.4 \times 10^{-13}$, low-density polyethylene at $7.3–9.7 \times 10^{-13}$, and high-density polyethylene at 2.4×10^{-13} g/m s Pa [51,55,56].

In general, decreases in the WVP were associated with a successful dispersal of the clay within the protein matrix, which distribution then produced a more tortuous path for the passage of water molecules through the film. Tunc et al. [18] observed an appreciable diminution in WVP upon adding 2.5% MMT to films composed of wheat gluten, and those authors attributed that drop to hydrophilic interactions between the gluten proteins and MMT, thus resulting in a lesser availability of the hydrophilic sites on the protein for the sorption of water molecules. These putative mechanisms could also apply equally well to the phenomenon of the solubility of protein films in water.

Since the WVP of a protein film depends on both the water solubility coefficient (β) and on the effective water diffusivity (D_{ef}) in the film [35] (Eq. (6)), the later measures were also determined (Table 3). At increases in the amount of clay both parameters declined progressively—β by 14% and D_{ef}, markedly so, by 78% at 10 g of MMT per 100 g of SPI—relative to the respective values for the unalloyed-protein film. These results evidenced that the diminution in WVP upon addition of the MMT to the protein matrix can be attributed to a decrease in both the water solubility coefficient and the diffusion of water throughout the film, with the latter effect being the more pronounced.

3.2.3. Mechanical properties

Fig. 4 shows the tension–deformation curves for both the pure-soy-protein and the nanocomposite films. The former film, the control, exhibited moderate properties: tensile strength up to about 3 MPa, elongation at break of about a 38%, and a Young's modulus of about 1.2 MPa; values that are found within the same range for other protein films in the literature [51,52,54,57–61]. With the addition of increasing amounts of clay a progressive enhancement in the resistance to breakage and in the modulus of elasticity was acquired along with a substantial decrease in the extent of elongation of the films relative to that of the control with pure protein—*e.g.*, at 10 g of MMT per 100 g SPI, the values

Table 4
GAB model constants (X_o, C, K) and coefficient of determination (r^2) for films of pure soy protein and of nanocomposites prepared with soy-protein isolate (SPI), and 5 and 10 g of montmorillonite (MMT) per 100 g of SPI. X_o=moisture content; C=Guggenheim constant associated to the sorption heat of the monolayer; K=constant associated to the sorption heat of multilayers.

MMT (g/100 g SPI)	X_o (g H_2O/g dry film)	C	K	r^2
0	0.1112	35.1699	0.9717	0.9913
5	0.0971	33.4347	0.9848	0.9901
10	0.0827	38.1817	0.9925	0.9892

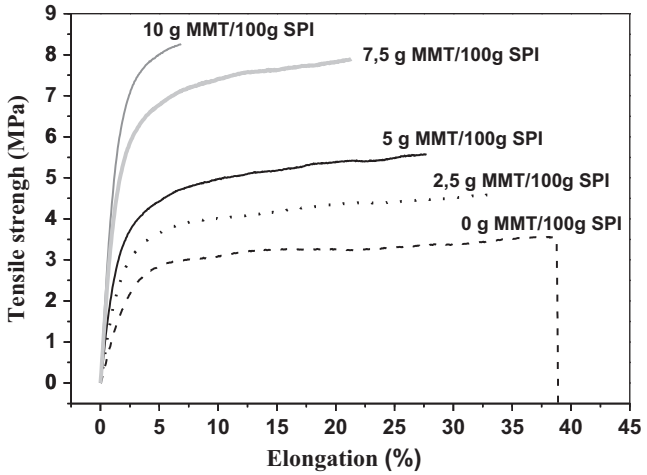

Fig. 4. Mechanical properties as from measured by traction of films prepared from soy protein isolated (0 g MMT/100 g SPI) and soy protein isolated with increasing concentrations of montmorillonite (MMT): 2.5, 5, 7.5, and 10 g MMT/100 g SPI.

attained were 137%, 327%, and 79% of the respective control parameters. The silicate layers of the clay thus provided a mechanical reinforcement for the protein matrix—no doubt owing to the strong interfacial interactions between the MMT and the latter—so that the nanocomposite films evidenced a notable improvement in the mechanical properties, especially with respect to Young's modulus. This interaction essentially results from the nature of the union between the soy proteins and the clay. Reports from as early as the first half of the twentieth century [62,63] had indicated that the complexes between MMT and proteins involved principally an interchange between the cationic groups of the amino-acid side chains (*e.g.*, the $-NH_3^+$ moieties) and Na^+ ions occupying the sites of interaction on the MMT surface. Other authors [17,57] much more recently attributed those improvements in mechanical properties to the strong electrostatic interactions and hydrogen bonding occurring between the soy proteins and the highly unordered MMT layers within the protein matrix. These interactions are critical for restraining the movement of the soy proteins, and that restriction is responsible for the majority of the resistance to traction in the form of a reinforcement of the modulus of elasticity of the nanocomposite films that in turn reduces the films' elongation under tensile stress. Also, as moisture content in composite films is lower as the MMT content increases (Table 3), there is less water available to plasticize the protein matrix, and this effect contributes to the increase in Young's modulus, tensile strength and lower elongation at break.

An optimal quantity of MMT for maximizing the mechanical properties of nanocomposite films with respect to yielding the highest rupture-free tension or modulus of elasticity has been reported [16,18]. This effect, and its optimization, is likely mediated by the formation of a progressive network of nanoclay that can eventually permeate the protein matrix at higher concentrations of MMT. In the present work the film with the highest MMT content was also the one that exhibited the optimal mechanical properties.

3.2.4. Thermal properties

Table 3 lists the T_g values obtained by DSC for the pure-protein and the nanocomposite films. The former films, with no MMT present, exhibited two glass-transition temperatures, at $-74\,^{\circ}C$ and $-40\,^{\circ}C$; the first attributable to a glycerol-rich phase and the second to a phase predominated by proteins [58,61]. In this regard, the literature contains T_g values for films made with protein from soybean [64], from wheat gluten plastified with glycerol or with mixtures of glycerol and sucrose [65], and from gelatin [58]; other references cite T_g values only after plastification with glycerol for proteins from milk whey [66], wheat gluten [67], and soybean [54]. The strong charge of the hydrophilic-amino-acid side chains of the soy proteins and their resulting polar interactions restrict the motility of those residues [68], but the intervention of glycerol within that microenvironment reduces those protein–protein interactions so as to generate a glass transition, and a corresponding T_g value, within the domains that have become rich in that plastifier.

After the addition of different concentrations of MMT to the soy-protein films, only the glass transition at around $-40\,^{\circ}C$, corresponding to the more protein-rich phase, was observed without alteration; the second transition at $-74\,^{\circ}C$ no longer occurred. The failure to observe that latter transition—it corresponding to the zone rich in glycerol—in the films containing MMT could suggest a redistribution of the plastifier within the protein matrix under those conditions because of the presence of the clay, but also point to the capacity of the components of those two transitional zones—the protein and the glycerol—to interact individually with the MMT. If the constancy of that remaining T_g is representative of a (bulk) protein matrix that is not altered upon the addition of the clay, then the failure of that component to become modified by a reduction in the water content of the films is an unexpected finding.

Hedenqvist et al. [69] reported that the T_g of nanocomposite films composed of whey protein and MMT rose by 5–10 °C after the addition of the latter to the formulation. Likewise, Rimdusit et al. [70] observed that the T_g of carboxymethylcellulaose–MMT nanocomposites increased from 176 to 182 °C upon augmenting the content of clay and attributed this rise to a restriction in the thermal movements of the methylcellulose because of the presence of the nanoclay. Similar increments in the T_g of bionanocomposites as measured by DSC can be cited in the literature [71–73].

3.2.5. Morphology of nanocomposite films

Fig. 5 shows the X-ray-diffraction spectra of natural MMT plus the pure-protein and MMT-nanocomposite films. The sodium–MMT curve reflected its characteristic crystallographic structure [74] with a peak of diffraction at around $2\theta = 72^{\circ}$ corresponding to an interlaminar space of $d_{001} = 1.2$ nm.

The intercalation of polymer chains into layers of clay usually increases the interlaminar space and in so doing produces a shift of the diffraction peak toward a lower angle—with the values of that angle being a function of the interlaminar space as given by the Bragg relationship (Eq. (7)). The term *exfoliated* refers to the failure to observe a peak in the X-ray-diffraction pattern because the space between the layers of pure clay is greater than between the layers of the intercalated film or because the nanocomposite films fail to possess an ordered structure [75].

The curve for the pure-protein film contained no transition within the range analyzed. The diffraction spectra of the nanocomposite films were without the characteristic MMT peak and also lacked the other peak at lower angles; those profiles exhibited only a widening and upward displacement of the basal curves upon approaching $2\theta = 2^{\circ}$, relative to the curve for the pure-protein film, a difference that became pronounced with increased concentrations of MMT. Although no well-defined shoulder was present in these latter spectra; nevertheless, that upward displacement might possibly be related to a certain degree of intercalation of the protein chains into the galleries of the layers of clay so as to cause a widening of the spacing between those nanocomposite sheets relative to that of the pure MMT. At the same time,

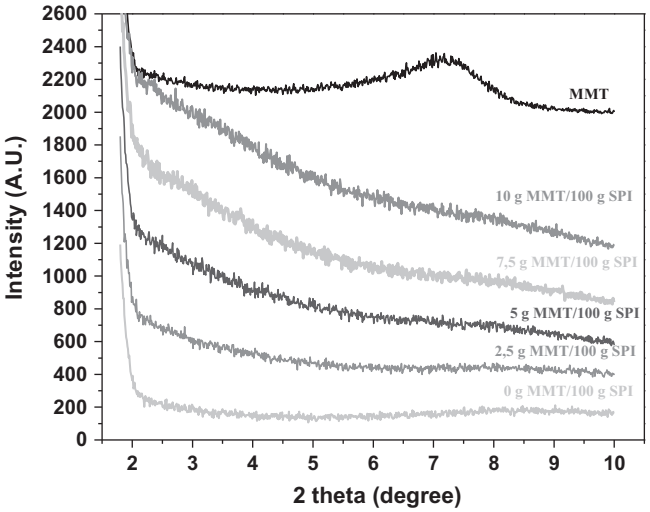

Fig. 5. X-ray-diffraction patterns of clay (pure montmorillonite) and nanocomposite films with 0, 2.5, 5, 7.5, and 10 g of montmorillonite per 100 g of soy-protein isolate (SPI).

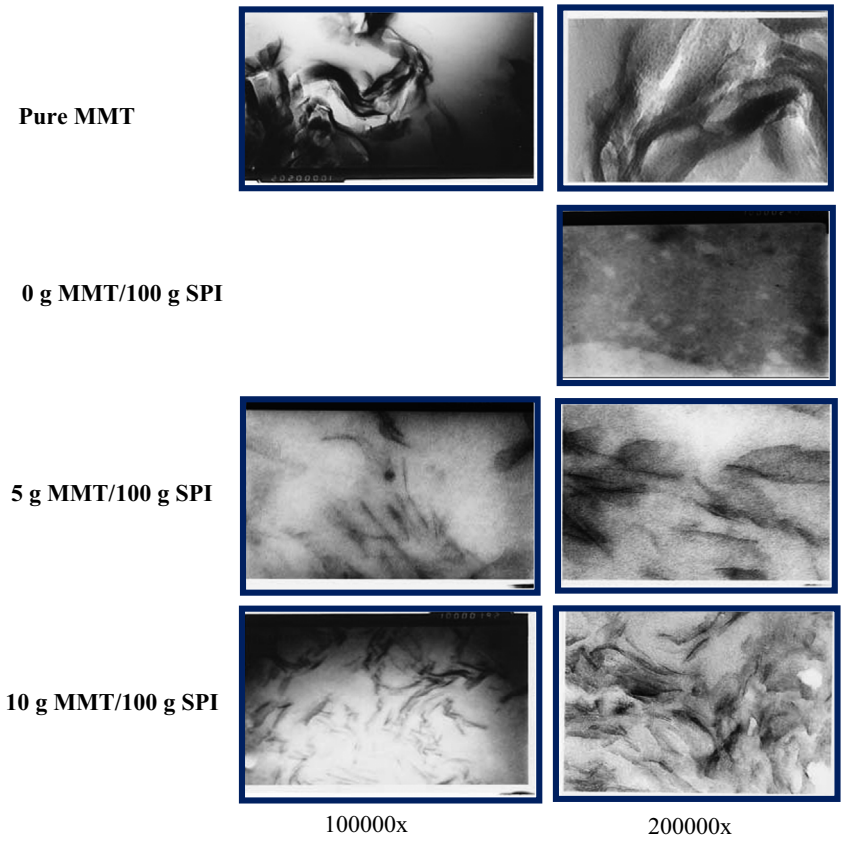

Fig. 6. Transmission electron microscopy of clay (pure montmorillonite) and nanocomposite films with 0, 5, and 10 g of montmorillonite per 100 g of soy-protein isolate (SPI).

certain layers may become separated from the rest and thus exfoliated, distributing themselves at random within the protein matrix [76]. Under such an interpretation, these curve displacements would likely be indicating a high degree of intercalation and/or exfoliation on the part of the clay within the protein matrix of the nanocomposites.

With an aim at verifying the X-ray evidence for the microstructure of the films, we also inspected them by transmission electron microscopy. Fig. 6 shows the micrographs of natural MMT and the films with either soy protein alone or soy protein plus MMT at concentrations of 5 and 10 g per 100 g of SPI. By this method the MMT is seen to be well dispersed throughout the protein matrix. Even though the layers of MMT still preserve their orientation in some measure, the tactoid ordering of those molecules has become markedly displaced by the soy proteins. These results therefore confirm the high degree of intercalation and consequent exfoliation (i.e., displacement) of the MMT achieved through the admixture of the nanocomposites that had been first evidenced by X-ray diffraction.

The improvements observed in the mechanical properties of the soy-protein films and in their resistance to water and heat degradation upon inclusion of MMT in their formulation is very likely related to this degree of intercalation and consequent exfoliation of the two components that results. This propitious restructuring of the admixture of soy protein and MMT, in turn, can be attributed to the use of the appropriate procedure to adequately disperse the clay as well as the beneficial interactions generated between the MMT and the soy protein within the films. That the uniform dispersion of the laminas of clay within the matrix increases the area of protein–clay contact further contributes to the efficient functionality of these nanocomposite films.

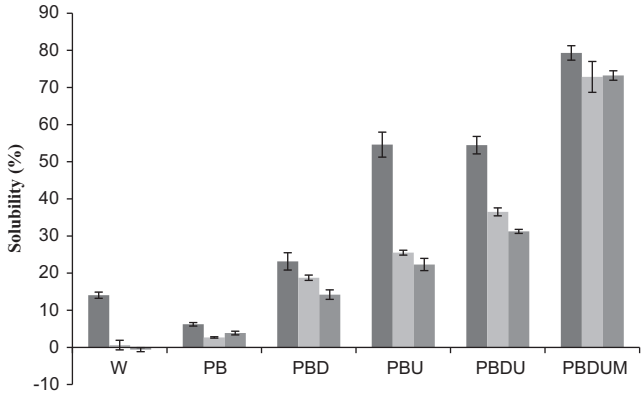

Fig. 7. Differential protein solubilization of films prepared with soy protein alone (■) or with 5 (▒) or 10 (▓) g of montmorillonite per 100 g of soy-protein isolate in buffers with different chemical activities: water (W), 0.1 M sodium phosphate buffer (PB), PB containing 0.1% (w/v) sodium dodecyl sulfate (SDS; PBD), PB containing 6 M urea (PBU), PB containing both 0.1% (w/v) SDS and 6 M urea (PBDU), and PBDU with 2.5% (v/v) ß-mercaptoethanol (PBDUM), all at pH 7.5. The content of solubilizable protein is expressed as a percent of the total amount of protein in the film. Values for each protein isolate are means ± standard deviations.

According to Majdzadeh-Ardakani et al. [77], the combination of mechanical mixing and ultrasound favors an efficient dispersion of the clay. Chen and Zhang [17] furthermore postulated that two types of chemical interactions between the soy proteins and the MMT in such nanocomposites were conducive to the intercalation and exfoliation of the MMT layers within the protein matrix: an electrostatic interation between the positively charged residues on the protein and the negative charges on the MMT layers and—as

has been already mentioned above—hydrogen bonding between the amino groups of the proteins and the Si–O groups of the clay.

With an aim at gaining a better understanding of the type and proportion of interactions involved in the stabilization of the protein network, we studied the differential solubility of the protein preparations used in the films in buffer systems known to possess the capacity of interfering with specific types of interactions (Fig. 7). These systems were: water (W), with the ability to dissolve free polypeptides not strongly linked to the protein matrix; phosphate buffer (PB), to affect protein electrostatic interactions; PB with SDS (PBD), to disrupt mainly hydrophobic interactions and also interact with proteins to increase their charge-to-mass ratio; PB with urea (PBU), to disrupt the structure of water, thus affecting hydrogen bonding as well as hydrophobic interactions; PBDU, to disrupt all the above-mentioned interactions and furthermore modify protein charge; and PBDUM, with β-mercaptoethanol, to cleave disulfide bonds (Fig. 7).

The control films with the soy-protein base were about 15% solubilized by water alone, which figure coincides with results obtained by other authors for the same protein isolate [48]. Under such conditions, what is dissolved and therefore quantified is the fraction of polypeptides that are neither covalently nor otherwise strongly bonded to the protein matrix. Upon solubilization with PB this degree of dissolution declined to less than 7% (a reduction of about 55%), probably because the buffer would favor ionic interactions among the proteins so as to produce a quasi-salting-out effect. The ionic detergent SDS in buffer PBD inhibits hydrophobic interactions among the polypeptide chains, while the urea in PBU modifies the capacity to form hydrogen bonds. The sharp increase in the protein solubilization in the presence of either of those compounds indicates that both hydrophobic interactions and hydrogen bonding participate in the stabilization of the structure of the film, with the greater contribution being the latter interaction since the degree of solubilization by PBU reached a level of 54% (as opposed to about half that value with PBD). The relative extent of these significant contributions to the integrity of the soy-protein film is further evidenced by treatment of the film with a buffer containing both those agents in combination, PBDU: there, the degree of solubilization did not exceed that seen in the presence of urea alone, thus indicating the predominance of the influence of hydrogen bonding. Exposure to the mercaptan ß-mercaptoethanol evidenced the presence of disulfide bridges: since the solubilization of the film protein was seen to increase up to 80% in the presence of the mercaptan in PBDUM buffer, that liability in the structure of the protein film would indicate the further role that disulfide bridging must play in the integrity of the soy-protein–film structure. References in the literature have corroborated that film-forming proteins with the capacity to combine through disulfide-bridging interactions generate more resistant and more greatly elongatable matrices [78] and that the formation of this type of interactions is favored when the proteins are denatured [79].

With the inclusion of MMT in the formulation the solubility of the proteins in the nanocomposites decreased significantly—and did so independently of the clay concentration—in all the buffers investigated relative to the respective control values in the absence of MMT. The pronounced decline in the protein solubilization in water is by now well established and constitutes evidence that the clay reduces the availability of free polypeptides. The lessening of the protein solubilization by urea in the buffers PBU and PBDU was likewise highly significant, being essentially additive in the latter buffer containing both urea and SDS. The differences in solubilization relative to that of the control films was finally much less pronounced in the presence of the reducing agent in buffer PBDUM, thus suggesting that the cleavage of disulfide bridges—besides favoring protein solubilization in the absence of that secondary structure—also enhances the efficiency of the other two reagents in their capacity to break protein–protein interactions.

These results would indicate that disulfide bridges evidently play a fundamental role in the stabilization of the structural matrix both in pure-protein films and in nanocomposites with MMT. Moreover, a major proportion of the moieties that are interacting through hydrogen bonding within the protein matrix in the absence of MMT become apparently involved in other types of interactions when the clay is present—perhaps with the clay itself—that are not easily destabilized.

4. Conclusion

This work demonstrates that MMT acts as a major strengthening component when added to soy-protein films since the strong interactions that exist between the proteins and the clay occur with the latter being thoroughly dispersed throughout the protein matrix and to a high degree intercalated by the protein components to the point of exfoliation. Also, the protein–protein, protein–glycerol, protein–water and glycerol–water interactions are modified by the presence of the layered silicate in the formulation, as it is demonstrated by differential solubilization of proteins of the nanocomposites films.

The improvements observed in the mechanical properties of the soy-protein films and in their resistance to water upon inclusion of MMT in their formulation is very likely related to the degree of intercalation and consequent exfoliation of the two components that results. This propitious restructuring of the admixture of soy protein and MMT, in turn, can be attributed to the use of the appropriate procedure to adequately disperse the clay as well as the beneficial interactions generated between the MMT and the soy protein within the films. That the uniform dispersion of the laminas of clay within the matrix increases the area of protein–clay contact further contributes to the efficient functionality of these nanocomposite films. In comparison with the control protein film Soy–MMT films showed an improvement in their resistance to mechanical deformation, protein solubilization in water and water vapor permeability, without affecting their visual appearance. The nanocomposite film with the highest content of clay analyzed conferred the most beneficial properties on the resulting nanocomposites.

Acknowledgments

The authors wish to thank the National Agency of Scientific and Technological Support of Argentina (SECyT, PICT 35036), and the DUPONT-CONICET prize for their financial support. The manuscript was translated into English from the original Spanish by Dr. Donald F. Haggerty, a retired career investigator and native English speaker.

References

[1] E.P. Giannelis, Polymer layered silicate nanocomposites, Adv. Mater. 8 (1996) 29–35.
[2] S.S. Ray, Rheology of polymer/layered silicate nanocomposites, J. Ind. Eng. Chem. 12 (2006) 811–842.
[3] S.S. Ray, M. Okamoto, Polymer/layered silicate nanocomposite: a review from preparation to processing, Prog. Polym. Sci. 28 (2003) 1539–1641.
[4] A. Sorrentino, G. Gorrasi, V. Vittoria, Potential perspectives of bio-nanocomposites for food packaging applications, Trends Food Sci. Technol. 18 (2007) 84–95.
[5] Y. Kojima, A. Usuki, M. Kawasumi, A. Okada, T. Karauchi, O. Kamigaito, Synthesis of nylon 6-clay hybrid by montmorillonite intercalated with ε-caprolactam, J. Polym. Sci. 31 (Part A) (1993) 983–986.

[6] Y. Kojima, A. Usuki, M. Kawasumi, A. Okada, T. Karauchi, O. Kamigaito, One pot synthesis of nylon 6-clay hybrid, J. Polym. Sci. 31 (Part A) (1993) 1755–1758.
[7] R.A. Vaia, E.P. Giannelis, Polymer melt intercalation in organically-modified layered silicates: model predictions and experiment, Macromolecules 30 (1997) 8000–8009.
[8] R.A. Vaia, S. Vasudevan, W. Krawiec, L.G. Scanlon, E.P. Giannelis, New polymer electrolyte nanocomposites: melt intercalation of poly(ethylene oxide) in mica-type silicates, Adv. Mater. 7 (1995) 154–156.
[9] Y. Kurokawa, H. Yasuda, A. Oya, Preparation of a nanocomposite of polypropylene and smectite, J. Mater. Sci. Lett. 15 (1996) 1481–1483.
[10] S.S. Ray, K. Yamada, M. Okamoto, K. Veada, Polylactide-layered silicate nanocomposite: a novel biodegradable material, Nano Lett. 2 (2002) 1093–1096.
[11] M. Avella, J.J. De Vlieger, M.E. Errico, S. Fischer, P. Vacca, M.G. Volpe, Biodegradable starch/clay nanocomposite films for food packaging applications, Food Chem. 93 (2005) 467–474.
[12] J.K. Pandey, K.R. Reddy, A.P. Kumar, R.P. Singh, An overview on the degradability of polymer nanocomposites, Polym. Degrad. Stab. 88 (2005) 234–250.
[13] H. Park, X. Li, C. Jin, C. Park, W. Cho, C. Ha, Preparation and properties of biodegradable thermoplastic starch/clay hybrids, Macromol. Mater. Eng. 287 (2002) 553–558.
[14] H. Park, W. Lee, C. Park, W. Cho, C. Ha, Environmentally friendly polymer hybrids. Part I. Mechanical, thermal, and barrier properties of thermoplastic starch/clay nanocomposites, J. Mater. Sci. 38 (2003) 909–915.
[15] B. Chiou, D. Wood, E. Yee, S.H. Imam, G.M. Glenn, W.J. Orts, Extruded starch–nanoclay nanocomposites: effects of glycerol and nanoclay concentration, Polym. Eng. Sci. 47 (2007) 1898–1904.
[16] V.P. Cyras, L.B. Manfredi, M.T. Ton-That, A. Vazquez, Physical and mechanical properties of thermoplastic starch/montmorillonite nanocomposite films, Carbohydr. Polym. 73 (2008) 55–63.
[17] P. Chen, L. Zhang, Interaction and properties of highly exfoliated soy protein/montmorillonite nanocomposites, Biomacromolecules 7 (2007) 1700–1706.
[18] S. Tunc, H. Angellier, Y. Cahyana, P. Chalier, N. Gontard, E. Gastaldi, Functional properties of wheat gluten/montmorillonite nanocomposite films processed by casting, J. Membr. Sci. 289 (2007) 159–168.
[19] P. Kumar, K.P. Sandeep, S. Alavi, V.D. Truong, R.E. Gorga, Effect of type and content of modified montmorillonite on the structure and properties of bionanocomposite films based on soy protein isolate and montmorillonite, J. Food Sci. 35 (2010) 46–56.
[20] M.R. Guilherme, L.H.Z. Mattoso, N. Gontard, S. Guilbert, E. Gastaldi, Synthesis of nanocomposite films from wheat gluten matrix and MMT intercalated with different quaternary ammonium salts by way of hydroalcoholic solvent casting, Composites: Part A 41 (2010) 375–382.
[21] P. Nayak, S.K. Sahoo, A. Behera, P.K. Nanda, P.L. Nayak, B.C. Guru, Synthesis and characterization of soy protein isolate/MMT nanocomposite film for the control release of the drug ofloxacin, World J. Nano Sci. Eng. 1 (2011) 27–36.
[22] J.N. Hay, S.J. Shaw, Organic–inorganic hybrids – the best of both worlds? Europhys. News 34 (2003) 15–18.
[23] C. Silvestre, D. Duraccio, S. Cimmino, Food packaging based on polymer nanomaterials, Prog. Polym. Sci. 36 (2011) 1766–1782.
[24] M.N. Emmambux, M. Stading, J.R.N. Taylor, Sorghum kafirin film property modification with hydrolysable and condensed tannins, J. Cereal Sci. 40 (2004) 127–135.
[25] R. Sothornvit, S. Hong, D.J. An, J.W. Rhim, Effect of clay content on the physical and anitimicrobial properties of whey protein isolate/organo clay composite films, LWT-Food Sci. Technol. 43 (2010) 279–284.
[26] M.B. Pérez-Gago, Protein-based films and coatings, in: E.A. Baldwin, R. Hagenmaier, J. Bai (Eds.), Edible Coatings and Films to Improve Food Quality, CRC Press, Taylor & Francis Group, LLC, Boca Raton, 2012, pp. 14–58.
[27] A. Gennadios, Protein Based Films and Coatings, CRC Press, Boca Raton, Florida, 2002.
[28] J. Irissin-Mangata, G. Bauduin, B. Boutevin, N. Gontard, New plasticizers for wheat gluten films, Eur. Polym. J. 37 (2001) 1533–1541.
[29] J.W. Rhim, J.H. Lee, H.S. Kwak, Mechanical and water barrier properties of soy protein and clay mineral composite films, Food Sci. Biotechnol. 14 (2005) 112–116.
[30] F. Song, D. Tang, X. Wang, Y. Wang, Biodegradable soy protein isolate-based materials: a review, Biomacromolecules 12 (2011) 3369–3380.
[31] N. Cao, Y.H. Fu, J.H. He, Preparation and physical properties of soy protein isolate and gelatin composite films, Food Hydrocolloids 21 (2007) 1153–1162.
[32] N. Gontard, S. Guilbert, J.L. Cuq, Water and glycerol as plasticizers affect mechanical and water vapor barrier properties of an edible wheat gluten film, J. Food Sci. 58 (1993) 206–211.
[33] A. Gennadios, T.H. McHugh, C.L. Weller, J.M. Krochta, Edible Coatings and Films to Improve Food Quality, in: J.M. Krochta, E.A. Balwin, M.O. Niperos-Carriedo (Eds.), Basel: Technomic Publishing, Lancaster, PA, 1994, pp. 201–277.
[34] T.P. Labuza, L.N. Ball, Moisture Sorption – Practical Aspects of Isotherm Measurement and Use, second ed., American Association of Cereal Chemists, St. Paul, MN, 2000.
[35] F.D.S. Larotonda, K.N. Matsui, P.J.A. Sobral, J.B. Laurindo, Hygroscopicity and water vapor permeability of Kraft paper impregnated with starch acetate, J. Food Eng. 71 (2005) 394–402.
[36] A.N. Mauri, M.C. Añón, Effect of solution pH on solubility and some structural properties of soybean protein isolate films, J. Sci. Food Agric. 86 (2006) 1064–1072.
[37] M.M. Bradford, A rapid and sensitive method for the quantification of microgram quantities of protein utilizing the principle of protein–dye binding, Anal. Biochem. 72 (1976) 248–254.
[38] R. Krishnamoorti, J. Ren, A.S. Silva, Shear response of layered silicate nanocomposites, J. Chem. Phys. 114 (2001) 4968–4973.
[39] E. Manias, G. Hadziioannou, G.T. Brinke, Inhomogeneities in sheared ultrathin lubricating films, Langmuir 12 (1996) 4587–4593.
[40] L. Petersson, K. Oksman, Biopolymer based nanocomposites: comparing layered silicates and microcrystalline cellulose as nanoreinforcement, Compos. Sci. Technol. 66 (2006) 2187–2196.
[41] G.A. Denavi, M. Perez-Mateos, M.C. Añón, P. Montero, A.M. Mauri, M.C. Gomez-Guillen, Structural and functional properties of soy protein isolate and cod gelatin blend films, Food Hydrocolloids 23 (2009) 2094–2101.
[42] J. Sharif, W.M.Z. Wan Yunus, K.Z.H. Mohd Dahlan, M.H. Ahmad, Preparation and properties of radiation crosslinked natural rubber/clay nanocomposites, Polym. Test. 24 (2005) 211–217.
[43] J.W. Rhim, K.W. Perry, Natural biopolymer-based nanocomposite films for packaging applications, Crit. Rev. Food Sci. Nutr. 47 (2007) 1–24.
[44] M.F. Huang, J.G. Yu, X.F. Ma, Studies on the properties of montmorillonite-reinforced thermoplastic starch composites, Polymer 45 (2004) 7017–7023.
[45] J.W. Rhim, Effect of clay contents on mechanical and water vapor barrier properties of agar-based nanocomposite films, Carbohydr. Polym. 86 (2011) 691–699.
[46] A. Casariego, B.W.S. Souza, M.A. Cerqueira, J.A. Teixeira, L. Cruz, R. Diaz, A.A. Vicente, Chitosan/clay films properties as affected by biopolymer and clay micro/nanoparticles concentrations, Food Hydrocolloids 23 (2009) 1895–1902.
[47] H. Almasi, B. Ghanbarzadeh, A.A. Entezami, Physicochemical properties of starch–CMC–nanoclay biodegradable films, Int. J. Biol. Macromol. 46 (2010) 1–5.
[48] P.R. Salgado, S.E. Molina Ortiz, S. Petruccelli, A.N. Mauri, Biodegradable sunflower protein films naturally activated with antioxidant compounds, Food Hydrocolloids 24 (2010) 525–533.
[49] S.Y. Cho, C. Rhee, Sorption characteristics of soy protein films and their relation to mechanical properties, LWT-Food Sci. Technol. 35 (2002) 151–157.
[50] B. Cuq, N. Gontard, J.L. Cuq, S. Guilbert, Selected functional properties of fish myofibrillar protein-based films as affected by hydrophilic plasticizers, J. Agric. Food Chem. 45 (1997) 622–626.
[51] A. Gennadios, C.L. Brandenburg, R.F. Weller, E. Testin, Effect of pH on properties of wheat gluten and soy protein isolate films, J. Agric. Food Chem. 41 (1993) 1835–1839.
[52] J.W. Rhim, A. Gennadios, A. Handa, C.L. Weller, M.A. Hanna, Solubility, tensile and color properties of modified soy protein isolate films, J. Agric. Food Chem. 48 (2000) 4937–4941.
[53] S.M. Martelli, G. Moore, S. Silva Paes, C. Gandolfo, J.B. Laurindo, Influence of plasticizers on the water sorption isotherms and water vapor permeability of chicken feather keratin films, Food Sci. Technol. 39 (2006) 292–301.
[54] G. Denavi, D.R. Tapia-Blácido, M.C. Añón, P.J.A. Sobral, A.N. Mauri, F.C. Menegalli, Effects of drying conditions on some physical properties of soy protein films, J. Food Eng. 90 (2009) 341–349.
[55] B. Cuq, N. Gontard, S. Guilbert, Proteins as agricultural polymers for packaging production, Cereal Chem. 75 (1998) 1–9.
[56] Y. Lin, K. Zhang, Z.M. Dong, L.S. Dong, Y.S. Li, Study of hydrogen-bonded blend of polylactide with biodegradable hyperbranched poly(ester amide), Macromolecules 40 (2007) 6257–6267.
[57] T.P. Aydt, C.L. Weller, R.F. Testin, Mechanical and barrier properties of edible corn and wheat protein films, Trans. Am. Soc. Agric. Eng. 34 (1991) 207–211.
[58] P.J.A. Sobral, F.C. Menegalli, M.D. Hubinger, M.A. Roques, Mechanical water vapor barrier and thermal properties of gelatin based edible films, Food Hydrocolloids 15 (2001) 423–432.
[59] S. Ou, Y. Wang, S. Tang, C. Huang, M.G. Jackson, Role of ferulic acid in preparing edible films from soy protein isolate, J. Food Eng. 70 (2005) 205–210.
[60] G.R.P. Moore, S.M. Martelli, C. Gandolfo, P.J.A. Sobral, J.B. Laurindo, Influence of the glycerol concentration on some physical properties of feather keratin films, Food Hydrocolloids 20 (2006) 975–982.
[61] D. Tapia-Blácido, A.N. Mauri, F.C. Menegalli, P.J.A. Sobral, M.C. Añón, Contribution of the starch, protein, and lipid fractions to the physical, thermal, and structural properties of amaranth (*Amaranthus caudatus*) flour films, J. Food Sci. 72 (2007) 293–300.
[62] L.E. Ensminger, J.E. Gieseking, The absorption of proteins by montmorillonitic clays, Soil Sci. 48 (1939) 467.
[63] L.E. Ensminger, J.E. Gieseking, The absorption of proteins by montmorillonitic clays and its effect on base-exchange capacity, Soil Sci. 51 (1941) 125.
[64] P. Chen, L. Zhang, S. Peng, B. Liao, Effects of nanoscale hydroxypropyl lignin on properties of soy protein plastics, J. Appl. Polym. Sci. 101 (2006) 334.
[65] G. Cherian, A. Gennadios, C. Weller, P. Chinachoti, Thermomechanical behavior of wheat gluten films: effect of sucrose, glycerin and sorbitol, Cereal Chem. 72 (1995) 1–6.
[66] N.B. Shaw, F.J. Monahan, E.D. O´Rioran, M. O'Sullivan, Effect of soya oil and glycerol on physical properties of composites WPI films, J. Food Eng. 51 (2002) 299–304.
[67] N. Gontard, S. Ring, Edible wheat gluten film: influence of water content on glass transition temperature, J. Agric. Food Chem. 44 (1996) 3474–3478.
[68] J. Zhang, P. Mungara, J. Jane, Mechanical and thermal properties of extruded soy protein sheets, Polymer 42 (2001) 2569–2578.
[69] M.S. Hedenqvist, A. Backman, M. Gallstedt, R.H. Boyd, U.W. Gedde, Morphology and diffusion properties of whey/montmorillonite nanocomposites, Compos. Sci. Technol. 66 (2006) 2350–2359.
[70] S.J. Rimdusit, D. Sorada, T. Siriporn, T.T. Sunan, Biodegradability and property characterizations of methylcellulose: effect of nanocompositing and chemical crosslinking, Carbohydr. Polym. 72 (2008) 444–455.

[71] P.R. Chang, F. Ai, A. Dufresne, J. Huang, Effects of starch nanocrystal-graft-polycaprolactone on mechanical properties of waterborne polyurethane-based nanocomposites, J. Appl. Polym. Sci. 111 (2009) 619–627.
[72] P. Krishnamachari, J. Zhang, A. Lou, J. Yan, L. Uitenham, Biodegradable poly (lactic acid)/clay nanocomposites by melt intercalation: a study of morphological, thermal, and mechanical properties, Int. J. Polym. Anal. Charact. 14 (2009) 336–350.
[73] H.M.C. Azeredo, L.H.C. Mattoso, R.J. Avena, G.C. Filho, M.L. Munford, D. Wood, T.H. McHugh, Nanocellulose reinforced chitosan composite films as affected by nanofiller loading and plasticizer content, J. Food Sci. 75 (2010) N1–N7.
[74] Y.C. Ke, P. Stroeve, Polymer-Layered Silicate and Silica Nanocomposites, first ed., Elsevier Science, Amsterdam, Netherlands, 2005.
[75] M. Alexandre, P. Dubois, Polymer-layered silicate nanocomposites: preparation, properties and uses of a new class of materials, Mater. Sci. Eng. 28 (2000) 1–63.
[76] M. Quilaqueo Gutiérrez, I. Echeverría, M. Ihl, V. Bifani, A.N. Mauri, Carboxymethylcellulose–montmorillonite nanocomposite films activated with murta (*Ugni molinae* Turcz) leaves extract, Carbohydr. Polym. 87 (2011) 1495–1502.
[77] K. Majdzadeh-Ardakani, A.H. Navarchian, F. Sadeghi, Optimization of mechanical properties of thermoplastic starch/clay nanocomposites, Carbohydr. Polym. 79 (2010) 547–554.
[78] J. Choi, R. Tamaki, S.G. Kim, R.M. Laine, Organic/inorganic imide nanocomposites from aminophenylsilsesquioxanes, Chem. Mater. 15 (2003) 3365–3375.
[79] N. Darby, T.E. Creighton, Disulfide bonds in protein folding and stability, in: B. A. Shirley (Ed.), Protein Stability and Folding: Theory and Practice, Humana Press Inc., Totowa, New Jersey, 1995, pp. 219–252.